ABES

Revista Brasileira de Ciências Ambientais
Brazilian Journal of Environmental Sciences

Application of response surface methodology in the optimization of the clarification and filtration system for the treatment of water from Açude Grande (PB), Brazil

Aplicação da metodologia de superfície de resposta na otimização do sistema de clarificação e filtração para o tratamento das águas do Açude Grande (PB), Brasil

Millena Dayse Barbosa da Silva[1], *Amanda Gondim Cabral Quirino*[1], *Laís Montenegro Teixeira* [1], *Elisângela Maria Rodrigues Rocha* [1], *Larissa Granjeiro Lucena*[1]

ABSTRACT

The deterioration of the environmental quality of the Açude Grande waters has worsened the water availability in the city of Cajazeiras (Paraíba state, Brazil) during drought periods. Thus, this study aimed to evaluate clarification followed by filtration to treat Açude Grande water. The research is innovative in applying optimization methods to conventional techniques for treating water sources considered unsuitable for human consumption in areas with limited water resources and economic and operational constraints. Thereby, the variables of aluminum sulfate concentration and pH were optimized based on the removal of turbidity and apparent color during the clarification stage (coagulation, flocculation, and decantation) using the central composite rotational design factorial plan associated with the response surface methodology. Subsequently, the filtration stage, consisting of a sand and gravel layer, was simulated at bench scale. The results showed that a coagulant dose of 60.0 mg.L^{-1} and a pH of 6 achieved the best removal of turbidity (67.3%) and apparent color (78.1%), bringing the turbidity parameter within the limits of the Ministry of Health Ordinance GM/MS No. 888/2021. As for the filtration process, it showed good efficiency in removing turbidity (>77.0%), apparent color (>70.0%), and biochemical oxygen demand (>46.0%) compared to the post-clarification sample. It is concluded that conventional treatment can potentially adjust the investigated parameters to organoleptic potability standards, with pre-oxidation being suggested to enhance the removal of organic matter.

Keywords: potability standard; factorial plan; conventional water treatment.

RESUMO

A deterioração da qualidade ambiental das águas do Açude Grande agravou a disponibilidade hídrica na cidade de Cajazeiras (estado da Paraíba, Brasil) em períodos de estiagem. Assim, o presente trabalho buscou avaliar a clarificação seguida de filtração para tratamento das águas do Açude Grande. A pesquisa é inovadora na aplicação de métodos de otimização em técnicas convencionais para o tratamento de mananciais considerados impróprios para o consumo humano, em localidades com recursos hídricos limitados e restrições econômicas e operacionais. Desse modo, as variáveis de concentração de sulfato de alumínio e pH foram otimizadas em função da remoção de turbidez e cor aparente na etapa de clarificação (coagulação, floculação e decantação), utilizando o planejamento fatorial do tipo delineamento composto central rotacional associado à metodologia de superfície de resposta. Posteriormente, a etapa de filtração, composta por uma camada de areia e brita, foi simulada em escala de bancada. Os resultados demonstraram que a dosagem do coagulante de 60,0 mg.L^{-1} e pH de 6 alcançaram a melhor remoção de turbidez (67,3%) e de cor aparente (78,1%), enquadrando o parâmetro turbidez nos limites da Portaria do Ministério da Saúde GM/MS n° 888/2021. Quanto ao processo de filtração, este apresentou uma boa eficiência na remoção dos parâmetros de turbidez (>77,0%), de cor aparente (>70,0%) e de demanda bioquímica de oxigênio (>46,0%) em comparação à amostra pós-clarificação. Conclui-se que o tratamento convencional tem potencial para adequar os parâmetros investigados aos padrões organolépticos de potabilidade, sendo sugerida a pré-oxidação para aumentar a remoção de matéria orgânica.

Palavras-chave: padrão de potabilidade; planejamento fatorial; tratamento convencional da água.

[1]Universidade Federal da Paraíba – João Pessoa (PB), Brazil.

Corresponding author: Millena Dayse Barbosa da Silva – Universidade Federal da Paraíba – Campus I – Castelo Branco – CEP: 58051-900 – João Pessoa (PB), Brazil. E-mail: millenadayse22@gmail.com

Funding: Federal University of Paraíba (UFPB), Coordination for the Improvement of Higher Education Personnel (CAPES, Coordenação de Aperfeiçoamento de Pessoal de Nível Superior-Brasil), Finance Code 001, and Paraíba State Research Support Foundation (FAPESQ, Fundação de Apoio à Pesquisa do Estado da Paraíba) under grant number 1868/2022.

Conflicts of interest: the authors declare no conflicts of interest.

Received on: 12/20/2024. Accepted on: 04/22/2025.

https://doi.org/10.5327/Z2176-94782411

Introduction

Analyzing water quality is a fundamental process for public health, ensuring it is free of contaminants and meets established quality standards. In conventional treatment, consisting of the coagulation, flocculation, decantation, filtration, and disinfection stages, the formation of flocs in coagulation-flocculation has a direct impact on the microbiological quality of the treated water (Xiao et al., 2024).

In this respect, optimizing water treatment using mathematical models helps to reduce the effects of seasonal variations and pollutant discharges, as well as making it possible to predict the best efficiency of processes without carrying out real experiments, which saves money and time (Chiavola et al., 2023; El-Taweel et al., 2023). From the perspective of optimizing the clarification-flocculation system in water treatment, the literature includes, in particular, studies by Chiavola et al. (2023), Husen et al. (2024), Rachid et al. (2024), Romphophak et al. (2024), and Trinh and Kang (2011).

Chiavola et al. (2023) optimized the dosage of the coagulant polyaluminum chloride in a water treatment plant (WTP), combining experimental modeling with a mathematical model based on historical data, to obtain a graph of the ideal dosage as a function of turbidity and flow rate. Husen et al. (2024) investigated linseed-based coagulants for treating water from the Awetu river in Ethiopia. The input variables potential hydrogen (pH), dosage, and agitation time were optimized using central composite rotational design (CCD), and the model was validated using analysis of variance (ANOVA).

On the other hand, Rachid et al. (2024) applied the design of experiments to identify the efficient dosages of aluminum sulfate, polymer, and carbon in removing turbidity from the water collected at the WTP inlet. Romphophak et al. (2024) developed a model based on Buckingham's Pi theorem to optimize the dosage of coagulants used to treat synthetic raw water with an in-line coagulation-flocculation system. Trinh and Kang (2011) used CCD and response surface methodology (RSM) to define the ideal combination of pH and coagulant dosage that results in the maximum removal of turbidity and dissolved organic carbon in water treatment from the Nakdong river in South Korea. The optimum condition was obtained by superimposing the contour curves.

When analyzing these studies, it can be seen that, except for the study by Trinh and Kang (2011), the others did not use the RSM to optimize treatment and did not superimpose the contour curves of the response variables. In addition, there were gaps in the field of application, as all the studies reviewed focused exclusively on improving the efficiency of water sources treatment already used for public supply.

In this context, it is apparent that the use of optimized conventional techniques in bodies of water classified as unfit for human consumption is still little explored, especially in regions where advanced treatment processes are challenging to implement on a full scale due to economic and operational restrictions. Therefore, the present research proposal fills a relevant gap in the literature by broadening the scope of studies and investigating the potential for reusing degraded water sources for specific uses.

The strategy is critical in the Northeast region of Brazil, where water resources are limited. According to the diagnosis of water and sewage services by the National Sanitation Information System (SNIS, Sistema Nacional de Informações sobre Saneamento), although Brazil has 12.0% of the planet's total freshwater, only 10% of this volume of water is available in the Northeast and Southeast regions to meet the multiple uses of the population (Brasil, 2023). Furthermore, data from the SNIS for 2022, referring to 5,451 municipalities, indicate that in the Northeast region, only 34.3% of the sewage generated receives adequate treatment (Brasil, 2023). As a result, more than 60.0% of effluent is discharged untreated, often into water sources, intensifying water scarcity.

Water availability in the Brazilian semiarid region is vulnerable to climatic conditions responsible for water level variations and hydrological processes of precipitation and evapotranspiration (Kolling Neto et al., 2024).

This study aimed to evaluate the efficiency of clarification combined with granular filtration in conventional treatment to bring the physicochemical and organoleptic parameters of the water from Açude Grande up to drinking water standards. The study area is located in the city of Cajazeiras, in Paraíba state inland, Brazil, in a scenario of reduced water availability and intense pollution, which has compromised its public supply capacity.

Regarding interdisciplinarity, the study encompasses sanitation and environmental technologies, with a view to the sustainable use of water from a degraded reservoir in a city in the Northeast inland.

Methodology

Collection and characterization of samples from the Açude Grande

The samples from the Açude Grande were collected during the dry season (absence of rain), following the procedures established by the American Public Health Association's Standard Methods for the Examination of Water and Wastewater (APHA et al., 2017). Two different geographical points of the spring were selected for sample collection (Figure 1), and 10 L of water was collected at each one. The containers were packed and transported to the Federal University of Paraíba Environmental Sanitation Laboratory.

Collection points A and B were selected based on their proximity to sources of pollution from urban occupation, which made it possible to analyze anthropogenic impacts on water quality. In addition, operational factors such as accessibility and researcher safety were taken into account, as large areas of the water body are inaccessible due to the dense presence of macrophytes, which is a limiting factor for collecting samples.

The characterization of the raw and samples after treatment included the physicochemical parameters defined in Table 1, based on the methodological procedures set out in the Standard Methods for the Examination of Water and Wastewater (APHA et al., 1992, 2017).

Factorial planning applied to the clarification stage of conventional treatment

The operating conditions for the clarification process (coagulation, flocculation, and decantation) were optimized using the CCD factorial model, which is associated with the RSM.

The following were chosen as input (independent) variables: aluminum sulfate concentration and pH. The effects of these variables were analyzed using the response (dependent) variables turbidity removal and apparent color removal.

The study range for the concentration of aluminum sulfate varied between 2.06 and 69.94 mg.L^{-1} and the pH from 5.59 to 8.41 (Table 2), based on the values established by Benakcha and Masmoudi (2024), Rachid et al. (2024), and Romphophak et al. (2024).

The coagulant used was liquid aluminum sulfate, with a stock solution prepared at a concentration of 5 g.L^{-1} and then diluted to obtain the desired concentrations. The Jar Test equipment (Figure 2), was used to simulate the coagulation, flocculation, and decantation stages.

The stirring speed for the fast and slow mixing stages was set at 100 rpm and 20 rpm, lasting 2 minutes and 15 minutes, respectively. The settling time was 30 minutes (Chiavola et al., 2023; Benakcha and Masmoudi, 2024; Husen et al., 2024).

After the decanting stage, the supernatant was collected, and apparent color and turbidity tests were carried out. According to Equation 1, treatment efficiency was defined by the value of R (%), in which X represents the value of the parameter analyzed.

$$R\ (\%) = \left(\frac{X_{Crude} - X_{Treated}}{X_{Crude}}\right) \quad (1)$$

The statistical treatment of the results was carried out using Statistica software (version 5.0, StatSoft), which enabled the development of a mathematical model capable of analyzing the influence of the input variables and their interactions on the response variables analyzed.

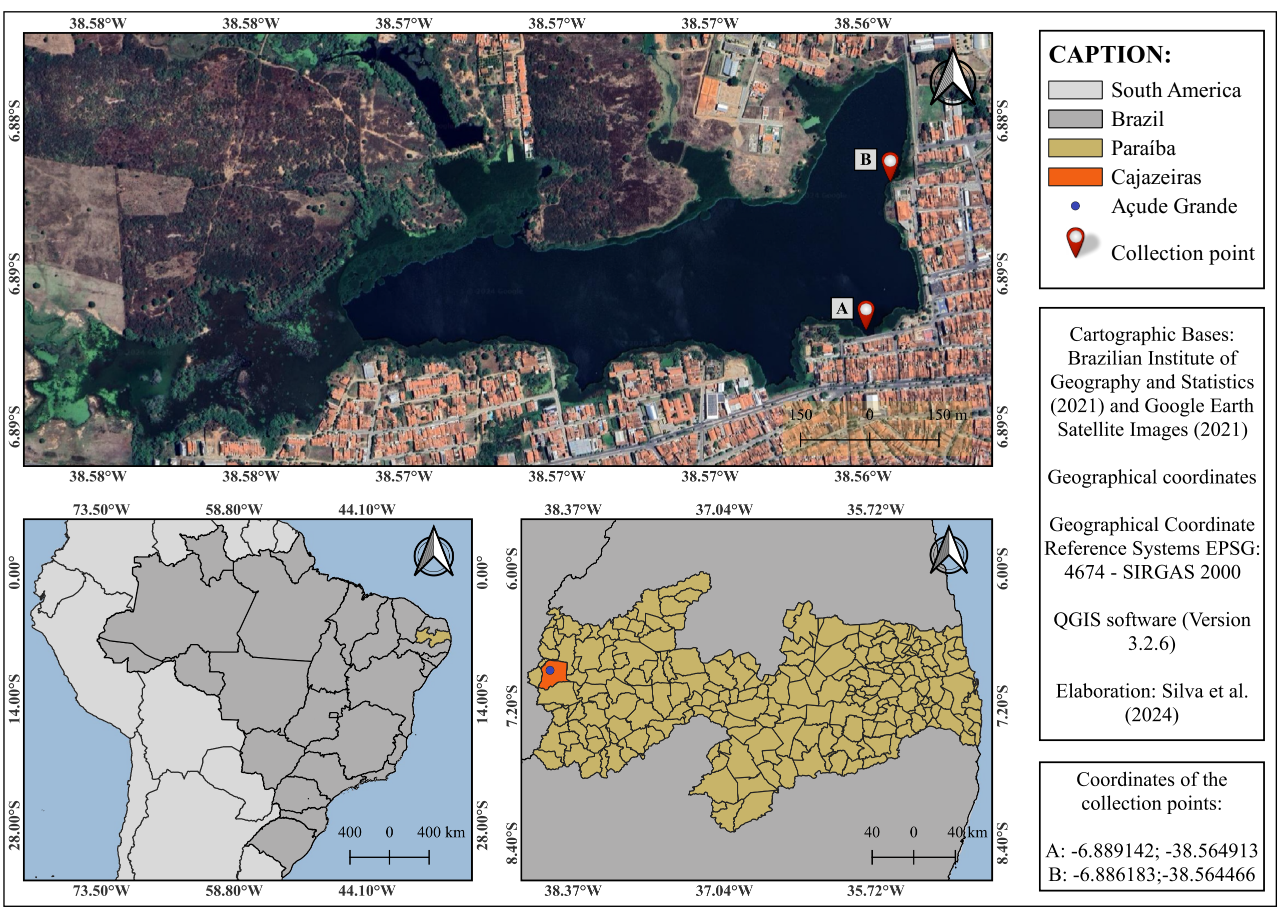

Figure 1 – Location map of the Açude Grande and collection points for the year 2023.

Thus, using the Pareto Chart, the first-order effects, second-order effects, and interactions between the factors on the response variables were determined with a significance level of α=0.05, identifying the statistically significant effects that should be included as terms in the model (Rodrigues and Iemma, 2014).

Subsequently, the accuracy of the model's fit to the experimental data was analyzed using the coefficient of determination (R^2). At the same time, the significance of the terms was assessed applying the F-test (Amiri and Sabour, 2014).

Finally, contour curves and response surfaces were drawn to determine the optimum conditions for the experiments.

Pilot-scale filtration system

A prototype single-layer filter was built with a height of 30 cm, a diameter of 100 mm, and an area of 0.00785 m^2. It was made of sand in three-grain sizes: fine, medium, and coarse, and a support layer of gravel No. 0. Figure 3 shows the filter structure.

The filter was assembled as follows: a. washing the transparent PET bottle with a volume of 2 L; b. washing the filter materials in running tap water and distilled water; c. removing the bottom of the bottle using a soldering iron and drilling holes in the removed bottom to produce the false bottom of the filter; d. opening the bottle cap to fit the nipple, 90° knee and tap assembly (diameter 1/2 inch), using thread sealant, durepoxi and white acetic silicone adhesive for sealing; e. using metal support with two hooks to support the structure and insert the false bottom into the bottle; f. assembling the layers of filtering material; and g. running tap water and distilled water through the assembled filter to remove any remaining impurities.

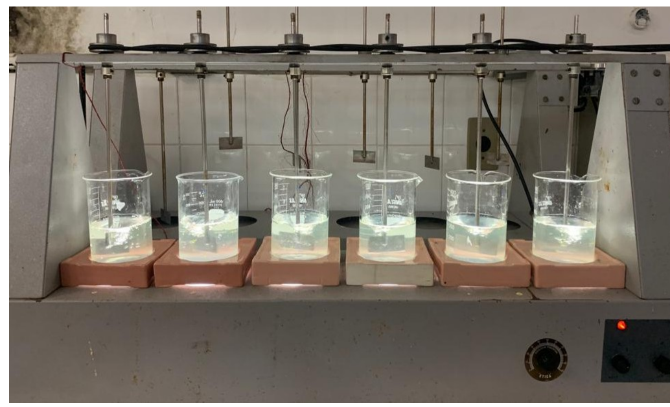

Figure 2 – Simulation of the coagulation, flocculation, and decantation stages in the Jar Test for the water from the Açude Grande.

Table 1 – Parameters and methods for characterizing the samples.

Parameters	Method	References
Total alkalinity	Titrimetric	APHA 2320 B
Chlorides	Argentometric	APHA 4500-Cl^- B
Electrical conductivity	Potentiometric	APHA 2510 B
Apparent color	Visual Comparison	APHA 2120 B
BOD_5	Respirometric	APHA 5210 D
COD	Closed reflux/ Colorimetric	APHA 5220 D
Total hardness	Titrimetric EDTA	APHA 2340 C
Nitrate	Salicylate	*APHA 4500-NO_3
Ammoniacal nitrogen	Direct Nesslerization Photometric	*APHA 4500-NH_3 C
pH	Electrometric	APHA 4500-H+B
Total Solids	Gravimetric	APHA 2540 G
Total fixed and volatile solids	Gravimetric	APHA 2540 G
Sulfates	Turbidimetric	APHA 4500-SO^2_4-E
Turbidity	Nephelometric	APHA 2130 B

Source: APHA et al. (2017).
BOD: biochemical oxygen demand; COD: chemical oxygen demand; EDTA: ethylenediaminetetraacetic acid; pH: potential hydrogen; APHA: American Public Health Association; *APHA et al. (1992).

Table 2 – Experimental design input variables for conventional treatment.

Variable	-1.41	-1	0	1	1.41
Coagulant concentration ($mg.L^{-1}$)	2.06	12	36	60	69.94
pH	5.59	6	7	8	8.41

It is worth noting that the heights of the filter layers were defined based on an adaptation of low-cost prototype filters developed by Sabogal-Paz et al. (2020) and Kisakye (2023). In this work, a single-layer filter was adopted, consisting of 5 cm of fine sand, 5 cm of medium sand, 5 cm of coarse sand, and 10 cm of gravel No. 0, with a free space of approximately 5 cm reserved at the top for the water to circulate.

Figure 3 – PET bottle prototype of the single-layer filter.

At the same time, a false bottom was used at the base to support the gravel.

After setting up the filter and determining the optimum condition for the clarification process, this condition was replicated in the Jar Test. Once the decantation time had elapsed, the supernatant was collected, reserving a volume of 4 L for characterizing the post-clarification sample and 4 L for the filtration test. In addition, the time taken for the water to percolate throughout the system was recorded, and the post-filtration samples were characterized.

Results and Discussion

Characterization of the Açude Grande samples

Table 3 compiles the results of the samples' physicochemical parameters, showing the maximum values established by Ordinance GM/MS No. 888/2021.

It can be seen (Table 3) that the chloride, total hardness, nitrate, ammonia nitrogen, and sulfate parameters for the two samples comply with the drinking water standards set out in Ordinance GM/MS No. 888/2021.

On the other hand, the apparent color and turbidity parameters for both samples exceeded the maximum permitted values, requiring appropriate treatment to correct these parameters. Therefore, to comply with Ordinance GM/MS No. 888/2021, it is necessary to achieve

Table 3 – Results of the physical-chemical characterization of the Açude Grande water in 2023.

Parameters	Collection (month)				Maximum value
	June (Dry)	SD	November (Dry)	SD	DW
Total alkalinity (mg $CaCO_3.L^{-1}$)	74.67	0.58	242.00	0.00	-
Chlorides (mg $Cl.L^{-1}$)	56.98	0.00	107.47	0.00	250
Electrical Conductivity ($\mu S.cm^{-1}$)	522.33	1.53	683.50	0.00	-
Apparent Color (uH)	80.00	0.00	75.00	0.00	15
BOD_5 (mg $O_2.L^{-1}$)	13.40	1.13	18.60	-	-
COD (mg $O_2.L^{-1}$)	124.50	3.54	80.66	0.62	-
Total hardness (mg $CaCO_3.L^{-1}$)	136.00	2.00	200.00	0.00	300
Nitrate (mg $N\text{-}NO_3.L^{-1}$)	0.00	0.00	0.00	0.00	10
Ammoniacal Nitrogen (mg N-NH3.L^{-1})	0.33	0.80	0.85	0.00	1.2
pH	7.22	0.01	7.47	0.06	-
Total Solids (mg.L^{-1})	0.33	0.01	0.48	0.01	-
Total Fixed Solids (mg.L^{-1})	0.074	0.01	0.12	0.01	-
Total Volatile Solids (mg.L^{-1})	0.26	0.02	0.36	0.01	-
Sulfates (mg $SO_4.L^{-1}$)	17.76	0.93	14.91	0.00	250
Turbidity (NTU)	14.84	1.12	22.50	0.71	5

*Hazen unit (mg Pt-Co.L^{-1}); SD: standard deviation; DW: drinking water (Ordinance GM/MS No. 888/21); BOD: biochemical oxygen demand; COD: chemical oxygen demand.

a turbidity removal of at least 66.30% for the first collection and a removal of around 77.78% for the second collection. Similarly, apparent color must be reduced by 81.20% for the first and 80.00% for the second collections.

The definition of suspended solids removal targets is fundamental in treatment, as it has an intrinsic relationship with the dosage of coagulants. Inadequate dosages do not reduce turbidity levels, which can cause blockages in the filtration units, while excessive dosages increase treatment costs (Chiavola et al., 2023).

Optimization of the clarification stage of conventional treatment

The experimental conditions for each test and the results obtained in terms of turbidity and apparent color removal efficiency are shown in Table 4. It is important to note that for the raw sample: turbidity was 14.84 NTU, and the apparent color was 80 uH.

Turbidity removal ranged from 14.00% (trial 5) to 67.00% (trial 3), while apparent color removal varied from 12.50% (trial 1) to 78.13% (trial 3). For both response variables, the experimental condition with a coagulant concentration of 60.00 $mg.L^{-1}$ and a pH of 6.00 (trial 3) resulted in the most significant removal of turbidity and apparent color. In this condition, the turbidity parameter (4.85 NTU) met the limit required by the drinking water ordinance (5.00 NTU).

Trials 6 and 7 also showed good removal of turbidity (>60.00%) and apparent color (>60.00%). However, it can be seen that in trial 6 (coagulant concentration of 69.94 $mg.L^{-1}$ and pH of 8.41), there was a higher consumption of coagulant compared to the other trials, which resulted in high costs in the treatment process. On the other hand, in test 7 (coagulant concentration of 36.00 $mg.L^{-1}$ and pH of 5.59), a more acidic pH was observed in the sample compared to test 3, requiring greater operational control and complexity in the WTP process.

Based on these discussions, the best experimental conditions for the clarification stages occurred at an aluminum sulfate concentration of 60.00 $mg.L^{-1}$ and a pH of 6.00 (test 3) within the study range.

The good performance of aluminum sulfate in the results obtained in Table 4 derived from the chemical interactions between the suspended particles and the aluminum ions. Before adding the coagulant, the colloidal particles are surrounded by negatively charged ions with a zeta potential between -40 and -30 mV, which are responsible for the repulsion forces that keep the particles in dispersion, preventing them from aggregating (Ferreira Filho, 2017).

When aluminum sulfate is added, the hydrolyzed species of the coagulant (Al^{+3}) introduce positively charged ions that attract negatively charged suspended particles, resulting in the destabilization of the suspended solids (Rachid et al., 2024; Romphophak et al., 2024). After the coagulation process, in slow mixing, the stirring speed and time parameters enable the suspended particles to aggregate and form larger flocs and, subsequently, the particles to sediment (El-Taweel et al., 2023).

In this respect, as chemical reactions depend on test conditions and the environment, maximizing the destabilization of the particles and forming flocs is essential. The multivariate analysis of the Pareto chart (Figure 4) determined the statistically significant effects on the removal of turbidity and apparent color, using Pure Error as the error term.

Table 4 – Results obtained in the clarification stage with aluminum sulfate in water treatment from the Açude Grande.

Essay	Input/ Independent variables				Response/ Dependent variables				End pH
	X_1		X_2						
	*Cod.	Real ($mg.L^{-1}$)	*Cod.	Real	Y_1 (NTU)	Y_1 (%)	Y_2 (uH)	Y_2 (%)	
1	-1.00	12.00	-1.00	6.00	12.53	15.50	70.00	12.50	7.33
2	-1.00	12.00	1.00	8.00	11.00	25.84	70.00	12.50	7.92
3	1.00	60.00	-1.00	6.00	4.85	67.30	17.50	78.13	7.39
4	1.00	60.00	1.00	8.00	8.90	39.99	30.00	62.50	7.78
5	-1.41	2.06	0	7.00	12.63	14.83	70.00	12.50	7.90
6	1.41	69.94	0	7.00	5.75	61.24	20.00	75.00	7.36
7	0	36.00	-1.41	5.59	5.53	62.70	30.00	62.50	7.35
8	0	36.00	1.41	8.41	8.37	43.59	60.00	25.00	7.95
9 (C)	0	36.00	0	7.00	8.03	45.84	40.00	50.00	7.77
10 (C)	0	36.00	0	7.00	8.43	43.14	40.00	50.00	7.85
11 (C)	0	36.00	0	7.00	7.97	46.29	40.00	50.00	7.85
12 (C)	0	36.00	0	7.00	8.17	44.94	50.00	37.50	7.75

*Coded value of the input variables in the factorial design.
X_1: coagulant concentration ($mg.L^{-1}$); X_2: pH; Y_1 (NTU): turbidity value; Y_1 (%): turbidity removal; Y_2 (uH): apparent color value; Y_2 (%): apparent color removal.

Figure 4 shows that the linear term of the coagulant concentration had the most significant and positive effect for the two response variables, indicating an increase in the removal of turbidity and apparent color at higher dosages of aluminum sulfate. El-Taweel et al. (2023) explained that adding aluminum sulfate to the aqueous solution increases the concentration of soluble aluminum, favoring the formation of hydroxocomplexes. These compounds react with each other to form hydroxometallic polymers. As a result, there is a reduction in the pH of the medium and greater production of aluminum hydroxide, which is responsible for retaining impurities.

However, if dosages are too excessive, there will be excess positive charges in the system, resulting in the polarity of the colloidal particles being reversed in a process known as charge reversal. In this phenomenon, the repulsion forces generated by positive charges prevent the particles from aggregating (Ferreira Filho, 2017).

The linear pH term was the second most significant effect for the apparent color removal variable and the third most considerable effect for the turbidity removal variable. In the responses, an adverse effect was observed, indicating that increasing the pH, in the study range of 5.59 to 8.41, reduces the removal of turbidity and apparent color. This can be attributed to the fact that, as stated by Ferreira Filho (2017), aluminum sulfate has its minimum solubility in aqueous media in the pH range of 5.50 to 7.50 when the solution is supersaturated. In this range, the coagulant reacts with the alkalinity of the aqueous medium and generates a gelatinous aluminum hydroxide precipitate (Rachid et al., 2024).

Benakcha and Masmoudi (2024) point out that, at pH 9.00, the predominant species of hydrolyzed aluminum are soluble anionic complex compounds with reduced formation of aluminum hydroxide. According to El-Taweel et al. (2023), aluminum sulfate is amphoteric and soluble at high or very low pH, with maximum efficiency in the zones of minimum solubility.

The polynomial mathematical models were determined after identifying the significant terms for each response variable (Table 5).

Table 5 shows that the turbidity and apparent color models fit the experimental data well (R^2>0.8).

In Table 6, ANOVA shows that the calculated F-value is greater than the tabulated F-value, indicating that the proposed model is statistically significant for both responses.

Myers et al. (2016) recommended that the calculated F-value be at least four to five times greater than the tabulated F-value for the model to be considered efficient at making predictions. Based on this, it is verified that the proposed models assist in making predictions within the study range.

It should be noted that the quality of the model's fit to the experimental data was also observed and predicted (Table 7). If the environmental conditions are unfavorable or some important variable has been overlooked, the data not explained by the model, the so-called residuals, will be significant (Trinh and Kang, 2011).

Table 7 reveals that the values observed experimentally and predicted by the model are close to each other for both viable responses.

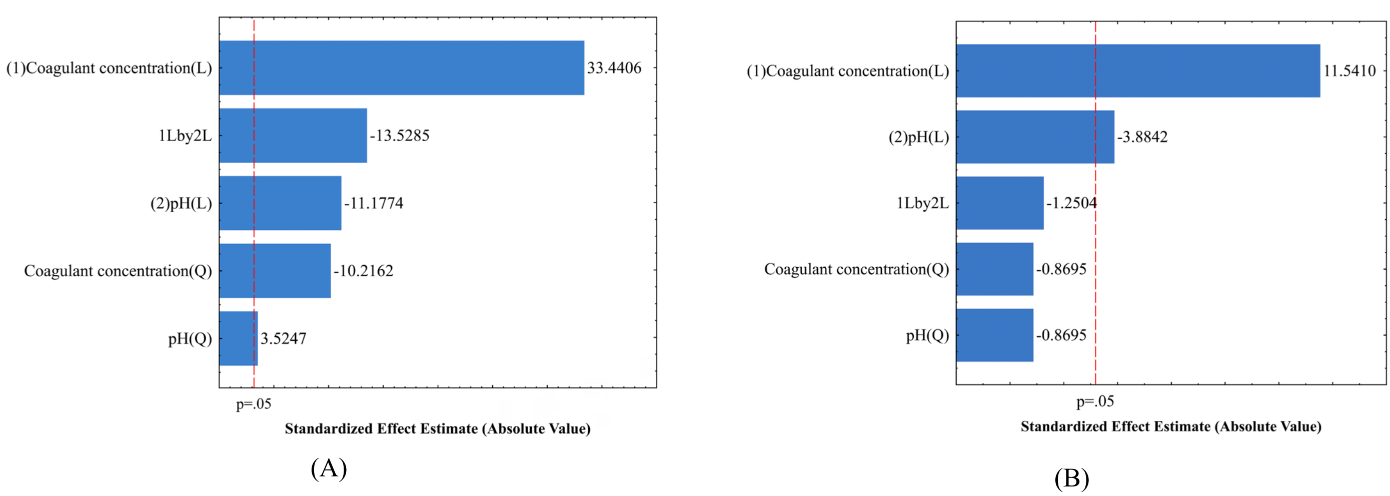

Figure 4 – Pareto chart for removal: (A) turbidity; (B) apparent color.

Table 5 – Regression models using aluminum sulfate for the dependent variables in the clarification stage.

Removal (%)	Regression model	R^2
Turbidity	$Y = 42.3928 + 4.1322X_1 - 0.0098X_1^2 - 18.5178X_2 + 1.9383X_2^2 - 0.3921X_1X_2$	0.9496
Apparent color	$Y = 65.83753 + 1.0626X_1 - 8.58288X_2$	0.9197

X_1 : aluminum sulphate concentration; X_2 : pH; R^2: coefficient of determination.

This confirms that the models can make good predictions in the study range and are considered satisfactory.

Finally, response surfaces were generated for the turbidity removal and apparent color removal variables, as shown in Figure 5.

Table 6 – Analysis of variance for the response variables of the conventional treatment clarification stages.

Removal (%)	Source of model variation	SS	DF	MS	F_C	F_T	F_C/F_T	R^2
Turbidity	Linear regression	3021.78	5	604.96	22.62	4.39	5.15	0.95
	Waste	160.47	6	26.74				
	Corrected total	3185.25						
Apparent color	Linear regression	5792.26	2	2896.13	51.50	4.26	12.09	0.92
	Waste	506.09	9	56.23				
	Corrected total	6298.36						

SS: sum squared; DF: degrees of freedom; MS: mean squares; (F_C): $F_{Calculated}$; (F_T): $F_{Tabeled}$.

Table 7 – Observed responses, predicted responses, and experimental error for the responses analyzed in the Açude Grande water clarification stage.

Essay	Turbidity removal			Apparent color removal		
	OV (%)	PV (%)	Error (%)	OV (%)	PV (%)	Error (%)
1	15.50	21.02	-5.51	12.50	27.09	-14.59
2	25.84	28.84	-2.99	12.50	9.93	2.57
3	67.30	72.73	-5.43	78.13	78.10	0.034
4	39.99	42.92	-2.92	62.50	60.93	1.57
5	14.83	10.56	4.27	12.50	7.94	4.56
6	61.23	57.08	4.15	75.00	80.08	-5.08
7	62.70	56.71	5.99	62.50	56.15	6.35
8	43.59	41.16	2.44	25.00	31.87	-6.87
9 (C)	45.84	45.06	-0.79	50.00	44.01	5.99
10 (C)	43.14	45.06	-1.91	50.00	44.01	5.99
11 (C)	46.29	45.06	1.24	50.00	44.01	5.99
12 (C)	44.94	45.06	-0.11	37.50	44.01	-6.51

OV: observed value; PV: predicted value.

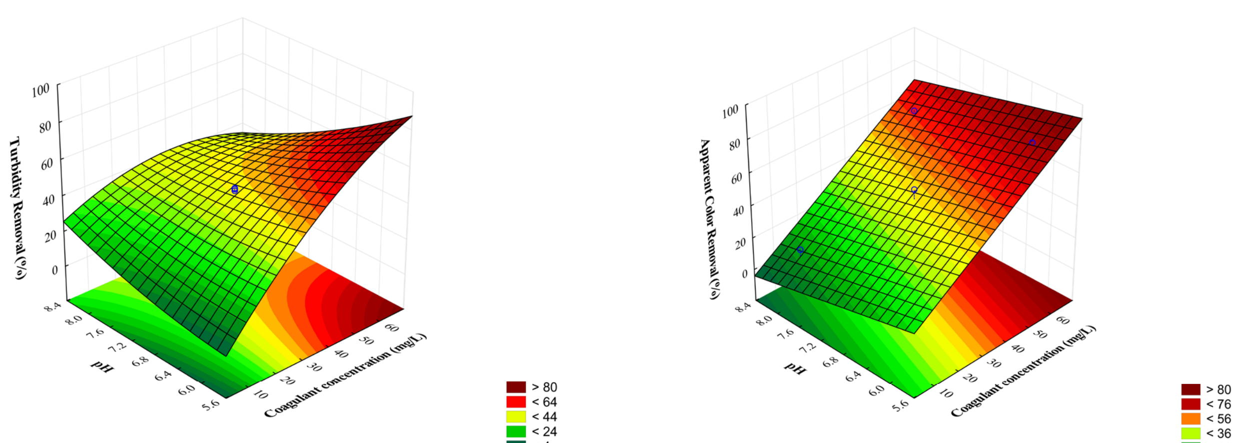

(A) (B)

Figure 5 – Response surface graph for removal of: (A) turbidity; (B) apparent color.

Figures 5A and 5B indicate that under conditions of minimum solubility in aqueous media, in the pH range of 5.50 to 7.50, greater turbidity removals are obtained for high dosages by keeping the pH constant. This phenomenon is probably due to the predominance of the sweeping mechanism in coagulation. In this process, aluminum sulfate must be added to saturate the suspended particles in the sweeping floc zone (Trinh and Kang, 2011). Therefore, when the solubility of the coagulant is exceeded, an aluminum hydroxide precipitate is formed, which promotes the destabilization of the particles (Ferreira Filho, 2017).

To meet the requirements of the drinking water ordinance, turbidity must be removed by at least 66.30% and apparent color by at least 81.20% (first collection). Considering that the drinking water standards refer to water that has undergone complete treatment and that filtration will still be used after the clarification stage to help achieve the color and turbidity standards, removal targets of at least 64.00% for turbidity and 76.00% for apparent color were set.

According to Rachid et al. (2024), the coagulant's performance is limited up to a critical point, at which additional dosages do not result in variations in turbidity. Thus, the ideal condition of aluminum sulfate concentration and pH, in which the necessary removal of turbidity and apparent color co-occurs, was obtained by superimposing the two contour curves of the dependent variables (highlighted in red in Figure 6).

From the analysis of Figure 6, it can be seen that the optimum region of investigation corresponds to the concentration range between 51.00 and 69.94 mg.L^{-1}, with a pH of 5.59 to 6.50. These results are in line with the study carried out by Trinh and Kang (2011).

Efficiency of the pilot-scale filtration system

The time taken to filter 4 L of the sample was 13 minutes, resulting in a filtration rate of 56.414 m^3/m^2/day, classified as intermediate between slow and fast filters. Table 8 describes the results of the physicochemical parameters of the raw samples (second collection),

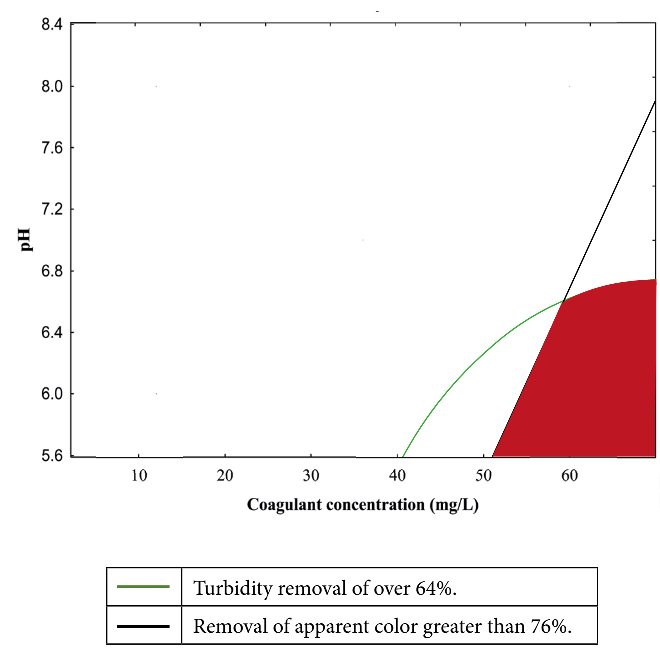

Figure 6 – Optimum region for turbidity removal and apparent color removal variables.

Table 8 – Characterization results for the Açude Grande samples: raw, post-clarification, and post-filter.

Parameters	RS	SD	PCS	SD	PFS	SD	DW
Total alkalinity (mg $CaCO_3$.L^{-1})	242.00	0.00	92.00	0.00	104.00	0.00	-
Chlorides (mg Cl.L^{-1})	107.47	0.00	109.97	3.54	107.47	0.00	250
Electrical Conductivity (µS.cm^{-1})	683.50	0.00	709.50	0.71	720.00	5.66	-
Apparent Color (uH)	75.00	0.00	25.00	0.00	7.50	0.00	15
BOD_5 (mg O_2.L^{-1})	18.60	-	13.35	3.47	7.10	-	-
COD (mg O_2.L^{-1})	80.66	0.62	60.70	0.18	10.70	-	-
Total hardness (mg $CaCO_3$.L^{-1})	200.00	0.00	200.00	0.00	208.00	1.41	300
Nitrate (mg N-NO_3.L^{-1})	0.00	0.00	0.00	0.00	0.00	0.00	10
Ammoniacal Nitrogen (mg N-NH3.L^{-1})	0.85	0.00	0.58	0.00	0.50	0.00	1.20
pH	7.47	0.06	6.38	0.03	6.85	0.06	-
Total Solids (mg.L^{-1})	0.48	0.01	0.52	0.02	0.54	0.01	-
Total Fixed Solids (mg.L^{-1})	0.12	0.00	0.10	0.02	0.12	0.00	-
Total Volatile Solids (mg.L^{-1})	0.36	0.01	0.42	0.04	0.41	0.02	-
Sulfates (mg SO_4.L^{-1})	14.91	0.00	170.20	3.11	169.50	6.22	250
Turbidity (NTU)	22.50	0.71	12.95	0.49	2.85	0.07	5

RS: raw sample; PCS: post-clarification sample; PFS: post-filter sample; SD: standard deviation; DW: drinking water (Ordinance GM/MS No. 888/21); BOD: biochemical oxygen demand; COD: chemical oxygen demand.

the post-clarification samples in the optimum condition, and the post-filtration samples, including the maximum permitted values for the organoleptic drinking standards set out in Ordinance GM/MS No. 888/2021.

Table 8 shows a significant reduction in the alkalinity and pH parameters between the raw and post-clarification samples and a significant increase in the sulfate content. According to Fleyfel et al. (2024), when aluminum sulfate is hydrolyzed in an aqueous solution, the hydrogen ions consume the water's alkalinity and reduce the medium's pH. In addition, adding sulphuric acid when adjusting the raw sample's pH to the optimum point's pH contributes to the increase in hydrogen ions in the solution. As for sulfate concentration, there are sudden variations in the parameter after the clarification stage because, according to Ferreira Filho (2017), the coagulant leaves a residual sulfate ion after reacting with the water.

The filtration process showed slight variation in alkalinity, pH, and sulfate compared to the post-clarification sample, as this process is dominated by physical-chemical interactions between the water and the constituent compounds of the sand, without the addition of reagents that significantly alter the chemical composition of the aqueous solution.

When analyzing the chemical oxygen demand (COD) parameter, 24.74% was removed after the clarification stage. On the other hand, filtration reduced the parameter by 82.37% compared to the post-clarification sample.

The clarification system's performance in removing organic matter results from the influence of pH on the formation of monomeric species obtained from the hydrolysis of aluminum sulfate. These compounds act to reduce turbidity and organic matter in the solution by interacting with their anionic sites and neutralizing the charge of the impurities, forming particles with lower solubility (Cañizares et al., 2009; Benakcha and Masmoudi, 2024).

This process was responsible for a 28.23% reduction in the biochemical oxygen demand $(BOD)_5$ parameter after the clarification stage. On the other hand, the filtration stage removed the BOD_5 parameter on the post-clarification sample by around 46.82%. Thus, the clarification system followed by filtration promoted a BOD_5 removal of 61.83%.

Azzam et al. (2022) analyzed raw water quality from four WTPs in the province of El-Monofeya in Egypt and obtained BOD values for the raw samples ranging from 4.60 to 7.00 mg $O_2.L^{-1}$. In turn, Sória et al. (2020) found that the average values of organic matter in the Pelotas Stream and the Quilombo Stream, located in Rio Grande do Sul, ranged from 4.60 to 5.10 mg $O_2.L^{-1}$ and from 1.70 to 3.70 mg $O_2.L^{-1}$, respectively, between 2007 and 2012. Hence, the result obtained for the BOD_5 concentration after filtration is higher than the range of raw water values found by the authors.

Regarding the turbidity parameter, Potability Ordinance GM/MS No. 888/21 establishes that the maximum value allowed to meet the organoleptic potability standards must equal 5.00 NTU in the distribution system's length or at the consumption point. However, daily monitoring requires that, after slow filtration, 95.00% of the samples have a turbidity of up to 1.00 NTU and 5.00% up to 2.00 NTU. In rapid filtration, 95.00% of post-filtration samples must reach 0.50 NTU, and 5.00% can reach 1.00 NTU (Brasil, 2021).

The clarification stage removed 42.44% of turbidity and 66.67% of apparent color. Compared to the post-clarification sample, the sand filter removed 77.90% of turbidity and 70.00% of apparent color. In this respect, the prototype filter met the organoleptic drinking standards for apparent color and turbidity but did not meet the turbidity standard for the post-filtration sample.

Therefore, to reduce the levels of organic matter and turbidity, it is recommended that the treatment be complemented with a pre-oxidation stage applied before coagulation, using hydrogen peroxide as an oxidant. The suggested technique is well-established and is frequently used by the Cajazeiras-PB WTP when significant changes in quality parameters are found due to seasonal variations.

Figure 7 presents the aesthetic appearance of the raw, post-clarification, and post-filtration samples.

The performance of the sand filter in removing the parameters of turbidity, apparent color, and organic matter stems from the efficiency of the clarification stage and the particle transport mechanism in the layers of the filter medium. Xiao et al. (2024) explain that the coagulation-flocculation process ensures the formation of stable flocs, uniform distribution, and large particle diameters. On the other hand, the sand grains in the filter medium have irregular sizes, varied shapes, a rough surface, and a porous nature (Shah et al., 2024). These factors allow the retention of flocs with diameters greater than the intergranular pores of the filter layer, with the particles adhering to the surface of the filter medium due to mutual adsorption, hydration reactions, and electrostatic forces (Ferreira Filho, 2017).

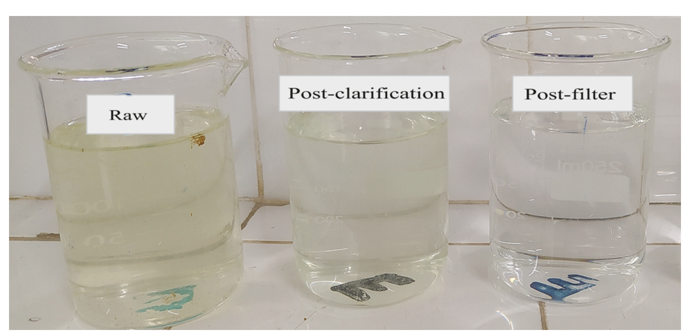

Figure 7 – Appearance of the Açude Grande samples: raw, post-clarification, and post-filter.

Conclusion

The study showed that the central composite rotational design factorial model, associated with the response surface methodology, performed well in removing suspended solids, guaranteeing an improvement in the aesthetic quality of the waters of the Açude Grande. This method makes the water treatment sustainable as it allows pH conditions of minimum solubility to be determined, as well as the effective dosages responsible for the best efficiency of the sand filters and for reducing costs.

Furthermore, the research showed that the models generated in the study domain are valid for modeling the best operating conditions for the clarification and filtration system for the waters of the Açude Grande. In this respect, the results show that the optimization of the conventional process can potentially adapt the physicochemical parameters investigated to drinking water standards, with the possibility of using the source for human supply or restricted uses in secondary activities. Therefore, using water bodies for human supply is subject to the analysis of biological tests, heavy metals, and organic compounds, which should be investigated in future research.

Finally, the proposal analyzed shows promising signs that could help mitigate the water source situation, which, due to intense pollution, has no purpose for use. The use of optimized methodologies has the potential to expand the field of application of conventional treatment, generating possible social and environmental benefits in regions with limited water resources and economic restrictions.

Authors' Contributions

Silva, M.D.B.: conceptualization, data curation, formal analysis, investigation, methodology, software, validation, visualization, writing – original draft, writing – review & editing. **Quirino,** A.G.C.: investigation, writing – original draft. **Teixeira**, L.M.: investigation, writing – original draft. **Rocha**, E.M.R.: supervision, validation, writing – review & editing. **Lucena**, L.G.: conceptualization, formal analysis, project administration, resources, supervision, validation, writing – review & editing.

References

American Public Health Association (APHA); American Water Works Association (AWWA); Water Environment Federation (WEF), 1992. Standard Methods for the Examination of Water and Wastewater. 18th ed. APHA, Washington, D.C.

American Public Health Association (APHA); American Water Works Association (AWWA); Water Environment Federation (WEF), 2017. Standard Methods for the Examination of Water and Wastewater. 23th ed. APHA, Washington, D.C.

Amiri, A.; Sabour, M.R., 2014. Multi-response optimization of Fenton process for applicability assessment in landfill leachate treatment. Waste Management, v. 34 (12), 2528-2536. https://doi.org/10.1016/j.wasman.2014.08.010.

Azzam, M.I.; Korayem, A.S.; Othman, S.A.; Mohammed, F.A., 2022. Assessment of some drinking water plants efficiency at El-Menofeya Governorate, Egypt. Environmental Nanotechnology, Monitoring & Management, v. 18, 100705. https://doi.org/10.1016/j.enmm.2022.100705.

Benakcha, M.; Masmoudi, T., 2024. Effect of adding biochar from prickly pear skin to aluminium sulphate to improve the coagulation-flocculation process during the elimination of humic substances present in the Laghrous drainage canal Water, Zab El-gharbi region (SE Algeria). Desalination and Water Treatment, v. 317, 100141. https://doi.org/10.1016/j.dwt.2024.100141.

Brasil, 2021. Ministério da Saúde – MS. Portaria n. 888, de 4 de maio de 2021. Diário Oficial da União, Brasília.

Brasil, 2023. Sistema Nacional de Informações sobre Saneamento. Diagnóstico temático serviços de água e esgoto: visão geral (Accessed March 25, 2024) at:. https://www.gov.br/cidades/pt-br/acesso-a-informacao/acoes-e-programas/saneamento/snis/produtos-do-snis/diagnosticos/DIAGNOSTICO_TEMATICO_VISAO_GERAL_AE_SNIS_2023.pdf.

Cañizares, P.; Jiménez, C.; Martínez, F.; Rodrigo, M.A.; Sáez, C., 2009. The pH as a key parameter in the choice between coagulation and electrocoagulation for the treatment of wastewaters. Journal of Hazardous Materials, v. 163 (1), 158-164. https://doi.org/10.1016/j.jhazmat.2008.06.073.

Chiavola, A.; Di Marcantonio, C.; D'Agostini, M.; Leoni, S.; Lazzazzara, M., 2023. A combined experimental-modeling approach for turbidity removal optimization in a coagulation flocculation unit of a drinking water treatment plant. Journal of Process Control, v. 130, 103068. https://doi.org/10.1016/j.jprocont.2023.103068.

El-Taweel, R.M.; Mohamed, N.; Alrefaey, K.A. Husien, S.; Abdel-Aziz, A.B.; Salim, A. I. Mostafa, N.G.; Said, L.A. Fahim, I.S.; Radwan, A.G., 2023. A review of coagulation explaining its definition, mechanism, coagulant types, and optimization models; RSM, and ANN. Current Research in Green and Sustainable Chemistry, v. 6, 100358. https://doi.org/10.1016/j.crgsc.2023.100358.

Ferreira Filho, S.S., 2017. Tratamento de água: concepção, projeto e operação de estações de tratamento. GEN/LTC, Rio de Janeiro, 463 p.

Fleyfel, L.M.; Matta, J.; Sayegh, N.F.; El Najjar, N.H., 2024. Olive mill wastewater treatment using coagulation/flocculation and filtration processes. Heliyon, v. 10 (22), e40348. https://doi.org/10.1016/j.heliyon.2024.e40348.

Husen, A.K.; Bidira, F.; Desta, W.H.; Asaithambi, P., 2024. COD, color, and turbidity reduction from surface water using natural coagulants: Investigation and optimization. Progress in Engineering Science, v. 1 (2-3), 100007. https://doi.org/10.1016/j.pes.2024.100007.

Kisakye, V., 2023. A bucket sand filter and Moringa Oleifera drinking water treatment hybrid system for rural households. Scientific African, v. 20, e01689. https://doi.org/10.1016/j.sciaf.2023.e01689.

Kolling Neto, A.; Ribeiro, R.B; Fraga, M.S.; Pruski, F.F., 2024. Estimating water balance in a Brazilian semiarid watershed using different spatial data. Journal of South American Earth Sciences, v. 140, 104930. https://doi.org/10.1016/j.jsames.2024.104930.

Myers, R.H.; Montgomery, D.C.; Anderson-Cook, C.M., 2016. Response Surface Methodology: Process and Product Optimization Using Designed Experiments. 4th ed. Wiley, Hoboken, New Jersey, 856 p.

Rachid, E.B.; Abderrahim, S.; Hafid, A.; Souad, R., 2024. Water treatment: aluminum sulfate, polymer, and activated carbon between efficacy and overdosing. Case of Oum Er-Rbia River, Morocco. Desalination and Water Treatment, v. 317, 100273. https://doi.org/10.1016/j.dwt.2024.100273.

Rodrigues, M.I.; Iemma, A.F., 2014. Planejamento de Experimentos e Otimização de Processos. 3th ed. Cárita Editora, Campinas, 358p.

Romphophak, P.; Chamnanmor, R.; Fagkaew, P.; Sairiam, S.; Painmanakul, P., 2024. Modelling the predictive analysis of turbidity removal efficiency in the in-line coagulation and flocculation process. Chemical Engineering Research and Design, v. 210, 301-310. https://doi.org/10.1016/j.cherd.2024.08.028.

Sabogal-Paz, L.C.; Campos, L.C.; Bogush, A.; Canales, M., 2020. Household slow sand filters in intermittent and continuous flows to treat water containing low mineral ion concentrations and Bisphenol A. Science of The Total Environment, v. 702, 135078. https://doi.org/10.1016/j.scitotenv.2019.135078.

Shah, A.; Arjunan, A.; Manning, G.; Batool, M.; Zakharova, J.; Hawkins, A.J.; Ajani, F.; Androulaki, I.; Thumma, A., 2024. Sequential novel use of Moringa oleifera Lam., biochar, and sand to remove turbidity, E. coli, and heavy metals from drinking water. Cleaner Water, v. 2, 100050. https://doi.org/10.1016/j.clwat.2024.100050.

Sória, M.; Tavares, V.E.Q.; Pinto, M.A.B.; Stumf, L.; Zarnott, D.; Bubolz, J.; Norenberg, B.G., 2020. Evaluation of physicochemical waterparameters in watersheds of southern Brazil. Revista Ambiente & Água, v. 15 (5), e2596. https://doi.org/10.4136/ambi-agua.2596.

Trinh, T.K.; Kang, L.S., 2011. Response surface methodological approach to optimize the coagulation–flocculation process in drinking water treatment. Chemical Engineering Research and Design, v. 89 (7), 1126-1135. https://doi.org/10.1016/j.cherd.2010.12.004.

Xiao, D.; Nan, J.; Zhang, X.; He, W.; Fan, Y.; Lin, X., 2024. Pilot-scale study of turbid particle evolutional/removal characteristics during coagulation-sedimentation-filtration (CSF): Effects of coagulant dosage and secondary dosing after breakage. Journal of Water Process Engineering, v. 68, 106325. https://doi.org/10.1016/j.jwpe.2024.106325.